Chem Biol Drug Des 2013; **82:** 167–177

Research Article

Penetratin and Derivatives Acting as Antibacterial Agents

Adriana D. Garro[1,2], Mónica S. Olivella[1], José A. Bombasaro[1], Beatriz Lima[3], Alejandro Tapia[3], Gabriela Feresin[3], Andras Perczel[4], Csaba Somlai[5], Botond Penke[5], Javier López Cascales[6], Ana M. Rodríguez[1,2] and Ricardo D. Enriz[1,2,*]

[1]*Departamento de Química, Facultad de Química, Bioquímica y Farmacia, Universidad Nacional de San Luis, Chacabuco 917, 5700, San Luis, Argentina*
[2]*IMIBIO-SL, CONICET, Chacabuco 917, 5700, San Luis, Argentina*
[3]*Instituto de Biotecnología, Facultad de Ingeniería, Universidad Nacional de San Juan, Av. Libertador General San Martín 1109 (O), CP 5400, San Juan, Argentina*
[4]*Protein Modeling Group HAS-ELTE, Institute of Chemistry, Eötvös Loránd University, Pázmány Péter sétány 1/A, H-1117, Budapest, Hungary*
[5]*Department of Medical Chemistry, University of Szeged, H-6720, Dóm tér 8, Szeged, Hungary*
[6]*Grupo de Bioinformática y Macromoléculas (BioMac) Aulario II, Universidad Politécnica de Cartagena, Campus de Alfonso XIII, 30203, Cartagena, Murcia, Spain*
**Corresponding author: Ricardo D. Enriz, denriz@unsl.edu.ar*

The synthesis, *in vitro* evaluation and conformational study of penetratin and structurally related derivatives acting as antibacterial agents are reported. Among the compounds evaluated here, two methionine sulphoxide derivatives (RQIKIWFQNRRM[O]KWKK-NH_2 and RQIKIFFQNRRM[O]KFKK-NH_2) exhibited the strongest antibacterial effect in this series. In order to better understand the antimicrobial activity obtained for these peptides, we performed an exhaustive conformational analysis using different approaches. Molecular dynamics simulations were performed using two different media (water and trifluoroethanol/water). The results of these theoretical calculations were corroborated using experimental CD measurements. The electronic study for these peptides was carried out using molecular electrostatic potentials obtained from RHF/6-31G(d) calculations. In addition, the non-apeptide RQIRRWWQR-NH_2 showed strong inhibitory action against the Gram-negative and Gram-positive bacteria tested in this study.

Key words: antibacterial activity, conformational study, methionine sulphoxide derivatives, penetratin, small-size peptides

Received 20 December 2012, revised 13 March 2013 and accepted for publication 7 April 2013

Small cationic peptides (1,2) are abundant in nature and have been described as 'nature's antibiotics' or 'cationic antimicrobial peptides'. They are found in every complex species (3) and are generally defined as having 12 to about 50 amino acids with 2–9 positively charged K or R residue and up to 50% hydrophobic amino acids. These peptides are folded in three dimensions, so that they have both a hydrophobic face comprising non-polar amino acid side chains, and a hydrophilic face of polar and positively charged residues: these molecules are amphipathic. The nature of the primary structure of cationic peptides appears to be of great significance for the activity, as a high content of cationic amino acids is a prerequisite for their initial association with negatively charged membrane components (4,5). The ratio between the cationic K and R residues influences membrane selectivity as the guanidino functionalities of R promote a more efficient interaction with eukaryotic membranes as compared with K. However, a high K content has been correlated with selectivity towards bacterial cells over eukaryotic cells (6). Another important factor reported for some antimicrobial peptides is related to their propensity to fold into a well-defined secondary structure (i.e. α-helix); thus, the antimicrobial activity of α-helical antimicrobial peptides depends on their propensity to form an α-helix (7,8).

Joliot *et al.* (9) reported that the 60 amino acid homeodomain of the Antennapedia protein of *Drosophila* was able to translocate over cell membranes. In order to understand the driving force for the internalization, the homeodomain was modified by site-directed mutagenesis leading to the discovery that its third helix was necessary and also sufficient for membrane translocation, which resulted in the development of a 16 amino acid-long cell-penetrating peptide (CPP) called penetratin (10). Thus, penetratin [**1**], a synthetic 16-amino acid peptide from the third helix of Antennapedia homeodomain (10,11), is a cationic amphipathic peptide and might penetrate cell membrane via a postulated 'inverted micelle' pathway. Penetratin has been proposed as a universal intracellular delivery vehicle (12). Thus, there are in the literature many articles reporting the cell-penetrating properties associated with penetratin (13–15). In addition, there is much information about the structural aspects of this interesting peptide as well (16,17). Regarding the antimicrobial activities, the antifungal activity of penetratin against *Candida albicans* (*C. albicans*) *and Cryptococcus neoformans* (*C. neoformans*) was

 doi: 10.1111/cbdd.12143

first reported by our group (18). Moreover, the antibacterial effects of this CPP have been demonstrated (19–22). Activity against both Gram-positive (19–21) and Gram-negative (21) bacteria has been reported for native penetratin. More recently, Bahnsen *et al.* (22) have reported the antimicrobial effects of penetratin and several derivatives of this CPP. It is interesting to remark that penetratin did not show cytotoxic effects against mammalian cells (20,22). Zhu and Shin (20) reported that two-stranded penetratin markedly increased cytolytic activity against human erythrocytes and NIH-3T3 mouse fibroblast cells without a significant effect on antimicrobial activity.

Peptides capable of both internalization into mammalian cells and killing of bacterial pathogens might well constitute potential candidates to search new structures as antibacterial agents. Thus, in this study, we tested first penetratin and other previously reported derivatives against several pathogenic bacteria. To better characterize the structure–antibacterial activity relationship of penetratin and derivatives, we also synthesized and tested new peptides structurally related to penetratin. The present search explored influences of amino acid substitutions and deletions on its antibacterial activity. In addition, to determine the tridimensional structure of peptides reported here, an exhaustive conformational analysis of penetratin and its derivatives was carried out using different approaches. Molecular dynamics (MD) simulations were carried out using two different media, water and a mixture of trifluoroethanol (TFE) and water trying to simulate the peptides inserted in the membrane. These theoretical simulations were corroborated using experimental circular dichroism (CD) measurements for the most representative compounds in this series. Thus, the ability of each approach to obtain the different conformations was tested and compared. An electronic study for these peptides was carried out using molecular electrostatic potentials (MEPs) obtained from RHF/6-31G(d) calculations. This conformational and electronic study was carried out in order to identify a topographical and/or substructural template, which may be the starting structure for the design of new peptides with the ability to inhibit bacterial growth. Finally, we extended our study synthesizing and testing new small-size peptides structurally related to penetratin. The principal goal was to obtain new small-size peptides, which were short in size but of full antibacterial potential.

Methods and Materials

Synthetic methods

The synthesis of the following peptides was already reported in previous works, details about the synthesis procedures can be obtained from their respective references: RQIKIWFQNRRMKWKK-NH_2 [**1**] (18), KKWKMRR NQFWIKIQR-NH_2 [**2**] (23), RWWKWWWWWRRWKWKK-NH_2 [**3**] (24), RQIRIWFQNRRMRWRR-NH_2 [**4**] (24), KQIKI WFQNKKMKWKK-NH_2 [**5**] (24), NRRMKWKK-NH_2 [**9**] (25), RQIRRWWQR-NH_2 [**10**] (26), RQIRRWWQW-NH_2 [**11**] (25) and RKFRRKFKK-NH_2 [**13**] (18).

Solid-phase synthesis of penetratin [**1**], RQIKIWFQNRRM-KWKK-NH_2, was carried out manually on a *p*-methylbenzhydrylamine resin (MBHA, 0.39 mmol/g) with standard methodology using Boc strategy. Side chain protecting groups were as follows: Tos for R and 2-chloro-Z for K. All protected amino acids were coupled in CH_2Cl_2 or CH_2Cl_2/DMF solvent mixture in a ratio of 1:1 (for Q and N) using DCC (2.5 equiv.) and HOBt (2.5 equiv.). Amino acid incorporation was monitored by Kaiser *et al.* (27) ninhydrin test. After coupling of the amino acid, Boc deprotection was effected using TFA/CH_2Cl_2 (1:1) for 5 min first then repeated for 25 min. The completed peptide resin was treated with liquid HF/dimethyl sulphide/anisole/indole (86:6:4:2) at 5 °C for 1 h. HF was removed, and the resulted free peptide was solubilized in 10% aqueous acetic acid and lyophilized. The crude peptide was purified by semi-preparative RP-HPLC on a Lichrosorb C-18 column (16 × 250 mm, 7 μm) with a linear gradient of acetonitrile 30–100%, 0.1% TFA in 70 min, 4 mL/min flow. The appropriate fractions were pooled and lyophilized. The purified peptide was characterized by HPLC and mass spectrometry using a Finnigan TSQ 7000 tandem quadrupole electrospray mass spectrometer. M + H calc.: 2244.3, found: 2244.5. Analytical HPLC conditions: column: Luna C-18, 5 μm, 4.6 × 250 mm, gradient: 30–50% AcN, 0.1% TFA in 10 min, 1.2 mL/min flow, 220 nm. R_t: 4.280 min. Same synthetic procedure and analytical HPLC conditions were applied for the peptide analogues as follows:

	Retention factor (min)	Gradient elution (%)
RQIKIWFQNRRM[O]KWKK-NH_2 [**6**]	5.794	25–40 (20 min)
RQIKIFFQNRRM[O]KFKK-NH_2 [**7**]	7.732	20–35 (15 min)
KQIKIWFQNKKM[O]KWKK-NH_2 [**8**]	10.099	20–40 (20 min)
RQIWRWWQW-NH_2 [**12**]	10.430	35–50 (15 min)
RQIRWQR-NH_2 [**14**]	6.203	20–30 (10 min)
RQIRW-NH_2 [**15**]	5.379	30–40 (10 min)

Peptides were dissolved in 50% aqueous methanol-0.5% acetic acid and analysed by TSQ 7000 triple-quad mass spectrometer (Finnigan). The instrument was equipped with an electrospray ion source (ESI), and the measurement was performed in positive mode. Spray voltage was 4.0 kV, capillary temperature set at 240 °C. The acquisition range was from 100 to 200 m/z. Data are as follows: [**6**] M + H = 2261.9; [**7**] M + H = 2183.9; [**8**] M + H = 2177.9; [**12**] M + H = 1443.6; [**14**] M + H = 1041.6; [**15**] M + H = 757.4.

Micro-organisms

The following strains were used: *Staphylococcus aureus* methicillin-sensitive ATCC 29213, *Staphylococcus aureus*

methicillin-resistant ATCC 43300, *Escherichia coli* ATCC 25922, *Escherichia coli* LM_1 (LM: Laboratorio de Microbiología, Facultad de Ciencias Médicas, Universidad Nacional de Cuyo, Mendoza, Argentina), *Escherichia coli* LM_2, *Pseudomonas aeruginosa* ATCC 27853, *Yersinia enterocolitica* PI (PI: Pasteur Institute), *Salmonella enteritidis* MI (MI: Malbrán Institute) and *Salmonella sp.* LM.

Antibacterial activity

Minimal inhibitory concentration (MIC) values were determined using the microbroth dilution method according to the protocols of the National Committee for Clinical and Laboratory Standards (28,29). All tests were performed in Mueller–Hinton broth, and cultures of each strain were prepared overnight. Micro-organisms suspensions were adjusted in a spectrophotometer with sterile physiological solution to give a final organism density of 0.5 McFarland scale ($1–5 \times 10^5$ CFU/mL). Stock solutions of peptides in DMSO were diluted to give serial twofold dilutions that were added to each medium to obtain final concentrations ranging from 10 to 1000 μg/mL. The final concentration of DMSO in the assay did not exceed 1%. The Cefotaxime ®Argentia Pharmaceutica antimicrobial agent was included in the assays as a positive control. The plates were incubated for 24 h at 37°. Minimal inhibitory concentration was defined as the lowest peptide concentration showing no visible bacterial growth after incubation time. Tests were performed in triplicate.

CD spectroscopy

Far-UV ECD data were acquired on a Jasco J810 dichrograph in 0.1-cm quartz cells; temperature controlled by a Peltier-type heating system. Each spectrum was obtained by averaging a total of four scans. Before each measurement, the sample in the cell was allowed to equilibrate for 5–10 min at the adjusted temperature. The solvent reference spectra were used as baselines, automatically subtracted from the peptide CD spectra. CD band intensities were expressed in mean residue ellipticity ($[\Theta]_{MR}$, deg $\times$ cm^2/dmol).

Computational methods

Molecular dynamics calculations

Molecular dynamics simulations were performed using two different molecular systems. On one hand, the conformational behaviour of peptides **2**, **6**, **7** and **8** in water was examined. On the other hand, a simulation with these peptides embedded in the TFE/water interface was performed. Molecular dynamics simulations and the trajectory analysis were carried out using the GROMACS 3.3 programs package (30) with the GROMACS (31,32) united-atoms force field. The peptides were embedded in a box containing the SPC water model (33) that extended to at least 10 Å between the solutes and the edge of the box. The total number of water molecules was 5679. Then, Cl^- ions were added to the systems by replacing water molecules in random positions, thus making the whole system neutral. The molecular system TFE/water biphasic environment consisted of 392 TFE molecules and 3682 water molecules (30% v/v); the size of the simulation box was 5.6 nm in the three spatial directions. Just then, the solvent (TFE and water) molecules were correctly localized into the box. An energy minimization and an NVT MD simulation of 20 ns long were performed to equilibrate the interfaces formed between solvent molecules. After the solvent stabilization was reached, a molecule of each peptide was embedded into the TFE/water interface. The positive charges of the peptides were neutralized with Cl^- ions replacing water molecules. An extra step of minimization of 1 ns long was performed before the production-MD simulation was started. The time step for the simulations was 2 fs. For long-ranged interactions, the particle-mesh Ewald (34) method was used with a 1.4 nm cut-off and a Fourier spacing of 0.12 nm. The MD protocol consisted of several preparatory steps: energy minimization using the conjugate gradient model (35), density stabilization (NVT conditions) and finally production of the MD simulation trajectory. All production simulations were performed under NPT conditions at 300.0 K and 1.0 bar, using Berendsen's coupling algorithm (36) for keeping temperature (τ_T = 0.1 ps) and pressure (τ_P = 0.5 ps) constant. The compressibility was 4.5×10^{-5}/bar. All coordinates were saved every 5.0 ps. The SETTLE (37) algorithm was used to keep water molecules rigid during MD simulations. The LINCS (38) algorithm was used to constrain all length bonds in the preparatory steps. However, no restrains were used in production-MD simulations. A length of 100 ns was taken in to account for all production-MD simulations.

Molecular electrostatic potentials

Quantum mechanics calculations were carried out using the GAUSSIAN 03 program.[a] We used the lowest energy conformations of peptides obtained from MD calculations. Subsequently, single-point *ab initio* (RHF/6-31G(d)) calculations were carried out. The electronic study was performed using MEPs (39,40). These MEPs were calculated using RHF/6-31G(d) wave functions, and MEPs graphical presentations were created using the MOLEKEL program.[b]

Results and Discussion

Antibacterial activity

We first tested penetratin (peptide **1** in Table 1), which showed just a moderate antibacterial effect. In particular, this peptide displayed antibacterial activity against *Escherichia coli* ATCC 25922, LM_1-*Escherichia coli*, LM_2-*Escherichia coli* and *Salmonella sp* (LM). In contrast, peptide **1** was devoid of any significant antibacterial activity against *Staphylococcus aureus* methicillin-sensitive ATCC 29213, *Staphylococcus aureus* methicillin-resistant ATCC 43300,

Table 1: Antibacterial activity of penetratin and derivatives

Compounds	MIC[a] (μM)								
	S.a (ms)	S.a (mr)	E.c.	LM_1-E.c.	LM_2- E.c.	Ps.a.	PI-Y.e.	MI-S.e.	S sp (LM)
RQIKIWFQNRRMKWKK-NH_2 **(1)**	>50	>50	25	40	25	>50	>50	>50	50
KKWKMRRNQFWIKIQR-NH_2 **(2)**	>50	>50	>50	25	25	>50	>50	25	25
R**WW**K**W**W**WWW**RR**W**KWKK-NH_2 **(3)**	>50	>50	>50	>50	50	>50	>50	25	50
RQI**R**IWFQNRRM**R**W**RR**-NH_2 **(4)**	>50	>50	25	25	25	>50	>50	25	50
KQIKIWFQN**KK**MKWKK-NH_2 **(5)**	>50	>50	>50	12.5	25	>50	>50	25	50
RQIKIWFQNRR**M[O]**KWKK-NH_2 **(6)**	>50	>50	12.5	12.5	25	>50	25	25	25
RQIKI**F**FQNRR**M[O]**K**F**KK-NH_2 **(7)**	>50	>50	50	12.5	12.5	>50	>50	12.5	25
KQIKIWFQN**KKM[O]**KWKK-NH_2 **(8)**	>50	>50	>50	25	50	>50	>50	25	50
NRRMKWKK-NH_2 **(9)**	>50	>50	>50	>50	>50	>50	>50	>50	>50
RQI**RR**WWQ**R**-NH_2 **(10)**	50	25	25	12.5	12.5	>50	25	25	25
RQI**RR**WWQW-NH_2 **(11)**	>50	>50	>50	40	>50	>50	>50	>50	30
RQIW**R**WWQW-NH_2 **(12)**	>50	>50	>50	50	>50	>50	>50	>50	50
RKF**RRK**F**KK**-NH_2 (**13**)	>50	>50	>50	>50	>50	>50	>50	>50	>50
RQIRWQR-NH_2 **(14)**	>50	>50	>50	>50	>50	>50	>50	>50	>50
RQIRW-NH_2 **(15)**	>50	>50	>50	>50	>50	>50	>50	>50	>50
Cef[b]	0.5	0.5	0.5	5	0.5	7.5	0.5	12.5	0.5

[a]The minimal inhibitory concentration (MIC) of the peptides were determined in μM (n = 3) for S.a (ms): *Staphylococcus aureus* methicillin-sensitive ATCC 29213, S.a (mr): *Staphylococcus aureus* methicillin-resistant ATCC 43300, E.c.: *Escherichia coli* ATCC 25922, LM_1-E.c.: LM_1-*Escherichia coli,* LM_2-E.c.: LM_2-*Escherichia coli,* Ps.a.: *Pseudomonas aeruginosa* ATCC 27853, PI-Y.e.: PI-*Yersinia enterocolítica,* MI-S.e.: MI-*Salmonella enteritidis,* S sp (LM): *Salmonella sp* (LM).
[b]Cefotaxime.

Pseudomonas aeruginosa ATCC 27853, PI-*Yersinia enterocolitica* and MI-*Salmonella enteritidis*. Earlier investigations on the antibacterial activity of penetratin against *E. coli* reported MIC values of: 25 μM (K12) (19), 32 μM (ATCC 25922) (22) and 2 μM (KCTC 1682) in a low nutrition 1% (w/v) peptone solution (21). It is clear that our present results are in complete agreement with those reported in references (19) and (22). Also, we extended our study measuring the MICs of penetratin towards LM_1-*E. coli* and LM_2-*E. coli,* which displayed a similar sensibility (40 and 25 μM, respectively; Table 1).

To study the structure–antibacterial activity relationship on this family of CPP, different penetratin derivatives and the effects of structural changes in their sequences were considered. Thus, we synthesized and tested peptides **2**–**5** (Table 1). It should be noted that compound **2** is the *retro–inverso* of penetratin, namely the position of the carbonyl and amino groups in each of the amide bonds of the polypeptide backbone was reversed, conferring a strong resistance to the peptide towards various proteases (41,42). The *retro–inverso* modification in peptides is a peptidomimetic approach able to transform short-lived biologically active peptides into much more stable molecules that retain their activity and are suitable for therapeutic use. Building the peptide in the reverse sense opposes the effect of the chirality inversion, thus leading to a high degree of topochemical equivalence, with the amino acid side chains properly arranged in space. In peptide **3**, the residues Q, I, F, N and M of peptide **1** were replaced by W, thereby increasing the number of hydrophobic residues. It has been demonstrated that the presence of a significant number of hydrophobic residues along the sequence of these cationic antimicrobial peptides is also of importance for their biological effect (17). Peptides **4** and **5** are analogues of **1** rich in R and K residues, respectively. In peptide **4**, all K residues of peptide **1** were replaced by R residues, while in peptide **5,** all R residues were substituted for K residues. All these derivatives (compounds **2**–**5**) showed an antibacterial activity slightly stronger than penetratin (Table 1). Note that compounds possessing in their sequence a larger number of cationic residues (peptides **4** and **5**) displayed better antibacterial effect in comparison with that obtained for peptides **3** (rich in W) and **2** (the *retro–inverso* of penetratin). Although derivatives **2**, **4** and **5** displayed an antimicrobial activity more potent than penetratin, they were just slightly better than this peptide. Our results are in good agreement with the antimicrobial effect against *E. coli* (ATCC 25922) reported for compounds **4** and **5** in reference (22). In addition, we obtained a significant antibacterial effect against LM_1-*E. coli* and LM_2-*E. coli* for both peptides.

On the basis of these results in the next step of our study, we attempted to obtain new peptides possessing more potent antibacterial activity. Previously, we reported that a particular combination of cationic and hydrophobic residues adopting a definite spatial ordering appears to be the key parameter for the transition from hydrophilic to hydrophobic phase, which could be a necessary step for these CPP to produce the antifungal activity (18,25,26). Now, we considered the possibility that a polarity increase at the M residue may contribute to obtain a better

electronic distribution in this moiety of the peptides which might facilitate the penetration of these compounds as well as their antimicrobial effects. In order to evaluate such situation, we performed a comparative conformational and electronic study of peptides **1** and **6**. In peptide **6**, M residue of peptide **1** was replaced by M-[O] (methionine sulphoxide or methionine sulphone). An evident change on the electronic distribution in the vicinity of M and M-[O)] residues and their respective influence zone was obtained from the MEPs calculated for compounds **1** and **6** (see the results obtained from MEPs calculations). Due to these theoretical results, peptide **6** was synthesized and tested. Interestingly, compound **6** displayed a marked increase in the antibacterial effect in comparison to that obtained for penetratin. Table 1 shows a comparison of the MIC values obtained against *E. coli* ATCC 25922, LM_1-*E. coli*, LM_2-*E. coli*, PI-*Y. enterocolitica*, MI-*S. enteritidis* and *Salmonella sp* (LM) for both peptides (**1** and **6**).

On the basis of the above results, peptides **7** and **8** possessing M-[O] residue in their structures were synthesized. Although both compounds displayed antibacterial effects, compound **7** was the most active peptide of this series. Peptide **7** showed antibacterial activity against LM_1-*E. coli*, LM_2-*E. coli*, MI-*S. enteritidis* and *Salmonella sp* (LM), being the first three the most sensible species. It is interesting to note that this compound yielded a significant inhibition percentage even at low concentrations (100% of inhibitory effect was observed at 12.5 μM). The inhibitory effect observed against *Salmonella sp* (LM) was lower than that obtained for MI-*S. enteritidis*, although it was still significant.

In summary, from the analysis of the antibacterial effects of peptides **1**–**8**, it is possible to infer that methionine sulphoxide derivatives exhibited the strongest activities in this series. In order to further understand the above experimental results, an exhaustive conformational and electronic study of the peptides reported here was performed using different approaches. These results are presented in the next section.

Conformational study of penetratin and derivatives

In order to better interpret the experimental results, a comparative conformational and structural study of this peptide series was carried out. To this end, two peptides without M-[O] residue in their structure (peptides **1** and **2**) and three peptides possessing M-[O] residue in their sequence (peptides **6**, **7** and **8**) were selected. Linear peptides are highly flexible and therefore to determine the biologically relevant conformations is not an easy task. In a previous study (18), we performed an extensive conformational study of penetratin (**1**) using molecular mechanics, simulated annealing and MD simulations. From those theoretical results, we concluded that the three methods predicted a helix-like structure as the preferred form for peptide **1** in water solution. Others studies have suggested that this peptide in solution is either partially α-helical (43,44) or has a partial β-hairpin structure (45). On the other hand, experimental CD studies have demonstrated that, in aqueous solution, penetratin (46,47) and analogues (23,24) existed predominantly as a random coil, but in a membrane-mimetic environment, these peptides displayed a clear tendency to form α-helical conformations. The structure determination from MD calculations may be used to monitor changes induced by the variation in the polarity of the molecular environment. Thus, peptides **2, 6, 7** and **8** were simulated using an extracellular matrix-mimetic environment and a membrane-mimetic environment. The aqueous solution simulated the extracellular matrix, while solutions containing TFE mimicked a membrane-like molecular environment. Molecular dynamics simulations were completed in water and in a mixture of TFE and water (3:7).

Peptide structure in highly aqueous medium

Figure 1 shows the change in the secondary structure during 100 ns of MD simulation in water for peptides **6** (a) and **7** (b). Simulations obtained for peptides **2** and **8** are shown in Figure S1 (in Supporting information). For peptides **2**, **6** and **8,** the initial conformation returned and remained stable in these simulations, suggesting that the starting helical structure was destroyed to form a mixture of α-helix, β-turn and bend in the structure at residues 2–15. Such a conformational behaviour was observed until the end of the simulation. The initial and final amino acids appear to have a random coil structure because of the flexibility of these residues. These results are closely related to those previously reported for penetratin (18). In contrast, peptide **7** displayed a different conformational behaviour. In this case, a mixture of coil, bend and turn conformations was formed after 70 ns of simulation. This mixture was observed until the end of the simulation.

Peptide structure in a low dielectric environment

Figure 1 shows the change in the secondary structure during 100 ns of MD simulation in TFE/water system for peptides **6** (c) and **7** (d). Simulations obtained for peptides **2** and **8** are shown in Figure S2 (in Supporting information). Peptide **1** was also included in this figure because it has been not previously reported in this environment. All the simulations performed using the TFE/water environment yielded very similar results. Residues 2–15 adopt a helix-like conformation, being the α-helix the predominant form. Once again the initial and final residues appear to have a random coil structure. Figure 2 shows a snapshot of the peptide **1**/TFE/water system at 80 ns of the MD simulation displaying the spatial orientation of this peptide in the membrane-like phase. Similar results were obtained for the rest of peptides reported here, being the results for peptide **1** representative of this series.

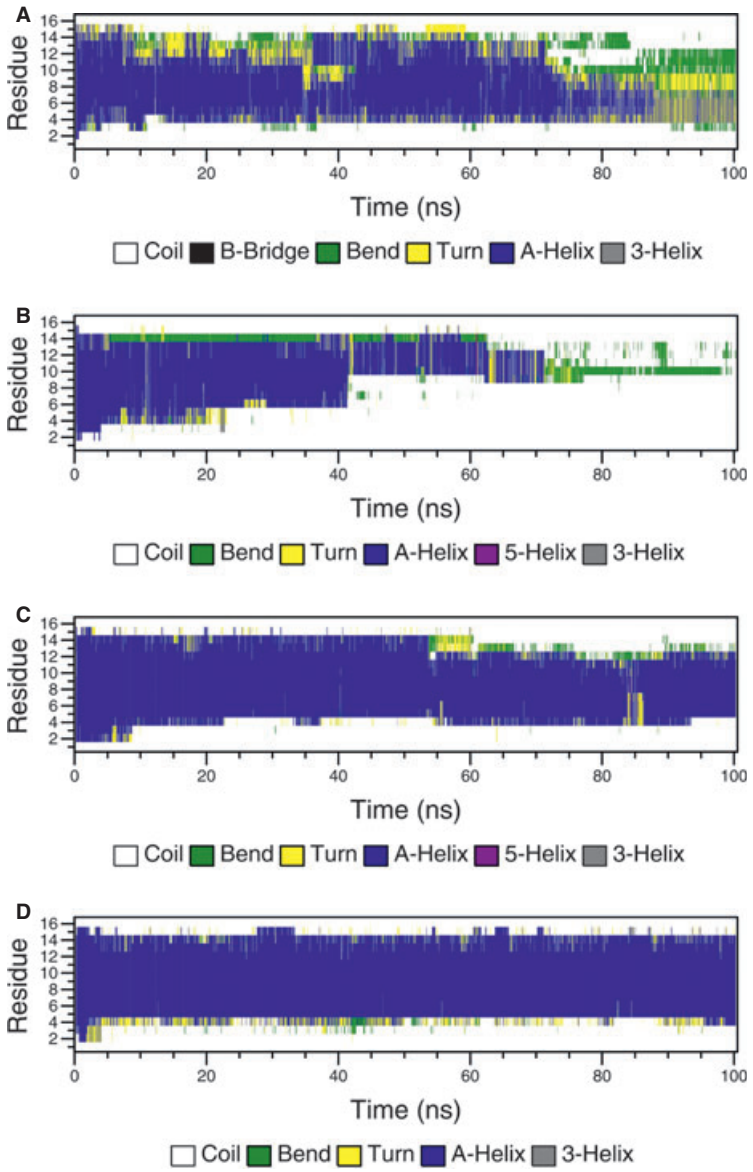

Figure 1: Change in the secondary structure during molecular dynamics simulations (100 ns): (A) in water for peptide **6**, (B) in water for peptide **7**, (C) in trifluoroethanol (TFE)/water system for peptide **6** and (D) in TFE/water system for peptide **7**.

Structure of peptides based on CD spectra

To corroborate the above theoretical results, in the next step, CD spectroscopic measurements were performed both in water and in a mixture of TFE and water (3:7) for peptides **7** and **8,** which possess M-[O] residue in their structures. They were measured at room temperature using the following conditions (pH adjusted by HCl/NaOH solutions); concentration: 0.023 mM; pH = 6.7. The exhaustive spectral analysis revealed that in water, peptides **7** and **8** existed predominantly as a random coil structure (Figure 3, black lines). The 'U'-type CD spectra reflected the presence of a very large number of different local conformations in a time average manner. Hence, in water, from the shape of these U-type CD curves, little characteristic secondary structure content could be extracted for any of these peptides (black lines). When the same peptides were recorded in the solvent mixture of 30% TFE and 70% H_2O, significant changes in the shape of both curves were observed. The CD curves of polypeptides **7** and **8** (see red lines in Figure 3A, B, respectively) had spectral features similar to those of a C-type CD curve. Thus, the 'red curves' most probably reflected a conformational ensemble composed of α- or 3_{10}-helix combined with type I/III β-turns plus some percentage of still unstructured (or highly mobile) backbone foldamers. These results indicate that in the presence of a considerable amount of TFE, peptides **7** and **8** adopt an increased amount of helical and/or type I/III β-turn secondary

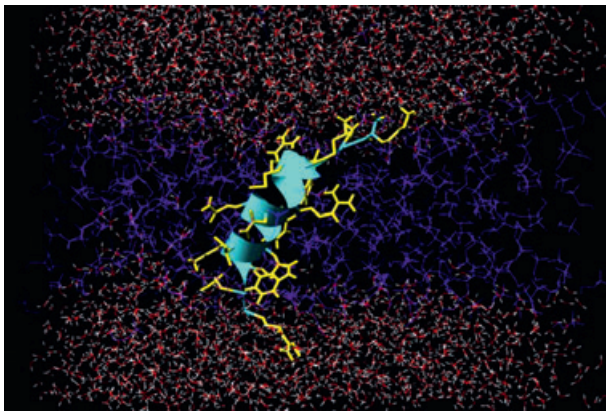

Figure 2: Snapshot of the location of peptide **1** taken at 80 ns of simulation in the trifluoroethanol (TFE)/water system.

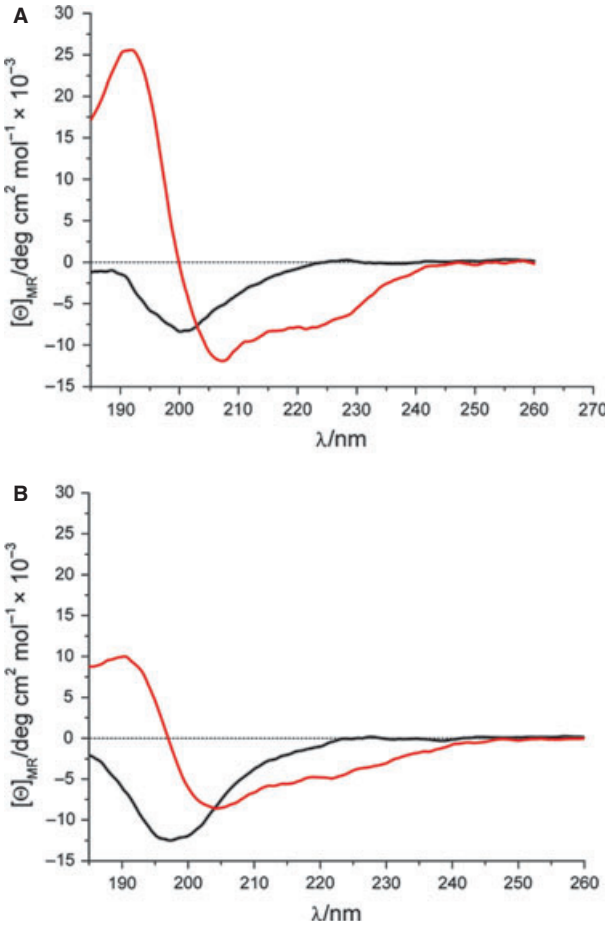

Figure 3: The CD spectra in water (black line) and in trifluoroethanol (TFE)/H_2O (3:7) (red curve) for (A) peptide **7** and (B) peptide **8**.

structure. These results are in agreement with those previously obtained for penetratin (44,45) (peptide **1**) and *retro–inverso* of penetratin (23) (peptide **2**). It is interesting to remark that these experimental measurements are

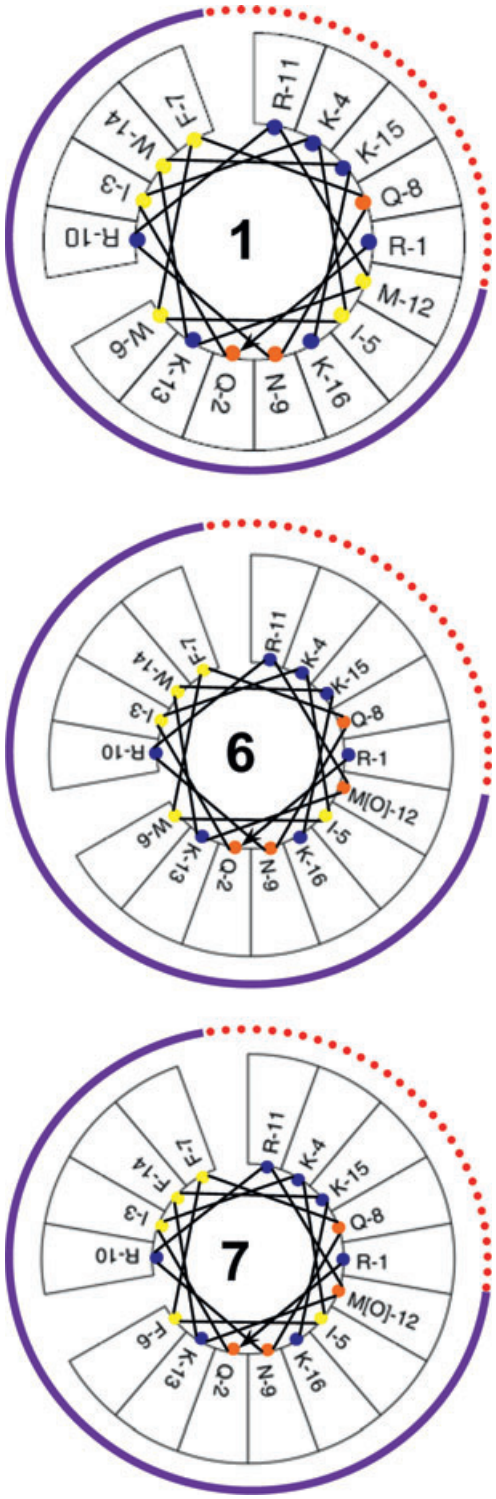

Figure 4: Edmundson wheel representations of peptides **1**, **6** and **7**. The number in the centre of the wheel corresponds to the peptide number. The 'charged' (CF) and 'non-charged' (NCF) faces are shown in red dotted lines and full violet lines, respectively. Positively charged amino acids are denoted with blue dots, the polar with orange and the hydrophobic with yellow. Similar Edmunson wheel representations were previously reported for peptide **1** (18).

also in complete agreement with our theoretical results giving an additional support to the MD simulations reported here.

To better characterize the spatial orientation of these peptides, Edmunson wheel representations of peptides **1**, **6** and **7** (Figure 4) and peptides **5** and **8** (Figure S2) were plotted. Previously, we reported that for these peptides, a balanced electronic distribution not 'too cationic' and not 'too hydrophobic' is necessary to produce the antifungal effect (18,24). The results obtained here indicated that such electronic distribution pattern appears to be necessary for the antibacterial activity as well. From Figure 4 and Figure S3, it is clear that the wheel representations obtained for peptides **5**–**8** were very similar, showing two clearly differentiated facades: the 'charged one' (denoted by a dash line in these figures) and a more extended 'uncharged one' (denoted by a full line). The first face identifies the cationic residues accounting for the mutual coulombic binding, and the second face is more extensive and is formed by hydrophobic and polar residues. The wheel representations obtained for the antibacterial peptides **5**–**8** were closely related to that previously reported for penetratin (peptide **1**) (18).

Molecular electrostatic potentials

The electronic study of peptides **1** and **6** was performed using MEPs (39,40). The fundamental application in this study was to observe whether the substitution of M by M-[O] introduced significant electronic changes in this portion of the peptide structures. The MEPs of peptides **1** and **6** are shown in Figure 5. Comparing both MEPs, it is possible to observe the different electronic distribution obtained for the zones located in the vicinity of M and M-[O] residues for compounds **1** and **6**, respectively. Note that M-[O] residue displayed a zone with potential values of about 0.133 el.au^{-3}, whereas the M residue shows a more positive green zone with potential values in the order of 0.306 el.au^{-3}, which clearly dominates this moiety. These results indicate that the replacement of M by M-[O] gives a more polarized potential. As previously remarked, it is reasonable to think that this different electronic distribution is operative to produce the biological response.

Searching novel small-size antibacterial peptides

Considering the premise 'the shorter the better', peptides composed of nine, eight, seven and five amino acids residues instead of 16 were synthesized (peptides **9**–**15**, Table 1). Cell penetration assays using cell cultures revealed that the C-terminal segment of penetratin (10-mer to 7-mer analogues) was necessary and sufficient for efficient cell membrane translocation (48). Thus, the 8-mer analogue of penetratin (peptide **9**) was synthesized in order to test its ability to inhibit bacterial growth. Unfortunately, this shortened penetratin analogue was completely inactive (Table 1). Taking into account, the potent antifungal activity previously obtained for small-size peptides containing nine amino acids residues (25,26), at this point, we decided to test two non-apeptides as possible antibacterial agents. To this end, peptides **10** and **11**, which were the strongest antifungal peptides of that series, were selected. Interestingly, peptide **10** displayed a significant antibacterial activity against all the species tested here except *P. aeruginosa*. It should be noted that this peptide was the only one in this group displaying antibacterial effect against *S. aureus*. Peptides **11** and **12** showed a markedly lower effect in comparison with peptide **10**. Peptides **11** and **12** only inhibited the growth of

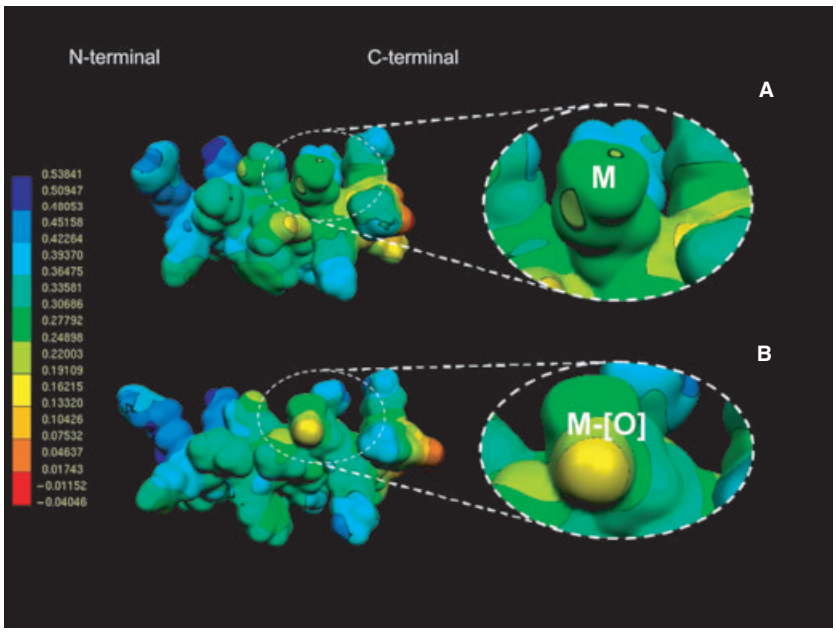

Figure 5: Electrostatic potential-encoded electron density surfaces obtained for peptides **1** (A) and **6** (B). The surfaces were generated with Gaussian 03 using RHF/6-31G (D) single-point calculations. The colouring represents electrostatic potential with red indicating the strongest attraction to a positive point charge and blue indicating the strongest repulsion. The electrostatic potential is the energy of interaction of the positive point charge with the nuclei and electrons of a molecule. It provides a representative measure of overall molecular charge distribution. The colour-coded is shown at the left. An enlarged view showing the zone at the vicinity of M and M-[O] residues is shown in a circle to the left.

E. coli and *Salmonella sp* (Table 1) displaying marginal effects. Thus, the low antibacterial activity of peptides **11** and **12** might be attributed to the inadequate balance between cationic and hydrophobic residues in their sequences. It should be noted that we gradually reduced the number of cationic R residues from peptide **10** (four R), peptide **11** (three R) and peptide **12** (two R). These results are in agreement with other studies suggesting that in the antimicrobial activity of short peptides, the overall composition with respect to cationic and lipophilic residues is more important than the order of amino acids (49,50). In fact, the non-apeptide **13** containing seven cationic amino acids (R or K) in its sequence, thereby decreasing the number of hydrophobic residues, was completely inactive. Finally, peptides **14** and **15** were also devoid of any antibacterial activity (Table 1).

Conclusions

In the present study, the synthesis and antibacterial effects of penetratin and analogues including derivatives containing methionine sulphoxide residues in their sequences are reported. Among the tested peptides, peptides **6** (RQIKIWFQNRRM[O]KWKK-NH_2) and **7** (RQIKIFFQNRRM[O]KFKK-NH_2) displayed the most interesting inhibitory effect against *E. coli* ATCC 25922, LM_1-*E. coli*, LM_2-*E. coli*, MI-*S. enteritidis* and *Salmonella sp* (LM). Our results support the use of the MD simulations for this type of peptides. Such simulations provide useful information about the preferred conformations and molecular flexibility of penetratin and derivatives, which might be useful to better understand the biological response of these peptides. Comparing the results obtained from the conformational analysis using the different approaches, we can conclude that in general, these methods predict a helical structure for penetratin and its derivatives at the TFE/water environment. These results are in agreement with the experimental results obtained from CD measurements. With regard to the electronic study, peptide **6** displayed a different electronic behaviour compared with native penetratin showing that a single amino acid substitution of M to M-[O] gives rise to substantial changes in the antibacterial activity. Taking into account that penetratin has been proposed as a universal intracellular delivery vehicle, the antibacterial activity displayed for peptides **6** and **7** is very interesting by itself, but it is also important considering its potential use as a carrier for other known antibacterial drugs. On the other hand, the possibility of these peptides, administered with well-known antibacterial drugs, to exert a synergic effect might be evaluated. In addition, we found that the non-apeptide (RQIRRWWQR-NH_2) having four R residues represents the most efficient motif for high antibacterial activity against the different bacteria tested in this study. Thus, we confirmed that the total amount and type of cationic and lipophilic residues used in short peptides is important for their antimicrobial activity. Our investigation of the antibacterial motif of small-size peptides regarding charge and lipophilicity/bulk opens the opportunity for development of novel and structurally diverse peptidemimetics. These compounds might provide a new source of antibacterial lead structures capable to overcome the pharmaceutical concerns such as high manufacturing costs, poor pharmacokinetic properties and low bacteriological efficacy.

Acknowledgments

This study is part of the Hungarian-Argentine Intergovernmental S&T Cooperation Programme. This research was supported by grants from Universidad Nacional de San Luis, CICITCA Universidad Nacional de San Juan and grants to R.D.E. (Agencia de Promoción Científica y Tecnológica de la Argentina PICT 2010-1832). This study was partly supported by grants from the Hungarian Scientific Research Fund (OTKA NK101072). R.D.E. and G.E.F. are researchers from CONICET (Argentina). A.D.G. and B.L. hold a fellowship from CONICET.

References

1. Hancock R.E.W. (1997) Peptide antibiotics. Lancet; 349:418–422.
2. Hancock R.E.W., Patrzykat A. (2002) Clinical development of cationic antimicrobial peptides: from natural to novel antibiotics. Curr Drug Targets Infect Disord;2:79–83.
3. Hancock R.E.W., Diamond G. (2000) The role of cationic antimicrobial peptides in innate host defences. Trends Microbiol;8:402–410.
4. Alves I.D., Bechara C., Walrant A., Zaltsman Y., Jiao C., Sagan S. (2011) Relationships between membrane binding, affinity and cell internalization efficacy of a cell-penetrating peptide: penetratin as a case study. PLoS ONE;6:e24096.
5. Letoha T., Keller-Pintér A., Kusz E., Kolozsi C., Bozsó Z., Tóth G., Vizler C., Oláh Z., Szilák L. (2010) Cell-penetrating peptide exploited syndecans. Biochim Biophys Acta;1798:2258–2265.
6. Park K.H., Nan Y.H., Park Y., Kim J.I., Park I., Hahm K., Shin S.Y. (2009) Cell specificity, anti-inflammatory activity, and plausible bactericidal mechanism of designed Trp-rich model antimicrobial peptides. Biochim Biophys Acta;1788:1193–1203.
7. Adão R., Nazmi K., Bolscher J., Bastos M. (2011) C- and N-truncated antimicrobial peptides from LFampin 265-284: biophysical versus microbiology results. J Pharm Bioallied Sci;3:60–69.
8. Lequin O., Bruston F., Convert O., Chassaing G., Nicolas P. (2003) Helical structure of dermaseptin B2 in a membrane-mimetic environment. Biochemistry;42: 10311–10323.

9. Joliot A., Pernelle C., Deagostini-Bazin H., Prochiantz A. (1991) Antennapedia homeobox peptide regulates neural morphogenesis. Proc Natl Acad Sci USA;88:1864–1868.
10. Derossi D., Joliot A.H., Chassaing G., Prochiantz A. (1994) The third helix of the Antennapedia homeodomain translocates through biological membranes. J Biol Chem;269:10444–10450.
11. Derossi D., Calvet S., Trembleau A., Brunissen A., Chassaing G., Prochiantz A. (1996) Cell internalization of the third helix of the Antennapedia homeodomain is receptor-independent. J Biol Chem;271:18188–18193.
12. Dupont E., Joliot A.H., Prochiantz A. (2002) Penetratin. In: Langel U., editor. Cell-penetrating peptides: processes and applications. Boca Raton, FL, USA: CRC Press; p. 23–51.
13. Tseng Y.L., Liu J.J., Hong R.L. (2002) Translocation of liposomes into cancer cells by cell-penetrating peptides penetratin and Tat: a kinetic and efficacy study. Mol Pharmacol;62:864–872.
14. Christiaens B., Grooten J., Reusens M., Joliot A., Goethals M., Vandekerckhove J., Prochiantz A., Rosseneu M. (2004) Membrane interaction and cellular internalization of penetratin peptides. Eur J Biochem;271:1187–1197.
15. Stewart K.M., Horton K.L., Kelley S.O. (2008) Cell-penetrating peptides as delivery vehicles for biology and medicine. Org Biomol Chem;6:2242–2255.
16. Clayton A.H.A., Atcliffe B.W., Howlett G.J., Sawyer W.H. (2006) Conformation and orientation of penetratin in phospholipid membranes. J Pept Sci;12:233–238.
17. Lensink M.F., Christiaens B., Vandekerckhove J., Prochiantz A., Rosseneu M. (2005) Penetratin-membrane association: W48/R52/W56 shield the peptide from the aqueous phase. Biophys J;88:939–952.
18. Masman M.F., Rodríguez A.M., Raimondi M., Zacchino S.A., Luiten P.G.M., Somlai C., Kortvelyesi T., Penke B., Enriz R.D. (2009) Penetratin and derivatives acting as antifungal agents. Eur J Med Chem;44:212–228.
19. Palm C., Netzereab S., Hällbrink M. (2006) Quantitatively determined uptake of cell-penetrating peptides in non-mammalian cells with an evaluation of degradation and antimicrobial effects. Peptides;27:1710–1716.
20. Zhu W.L., Shin S.Y. (2009) Antimicrobial and cytolytic activities and plausible mode of bactericidal action of the cell penetrating peptide penetratin and its Lys-linked two-stranded peptide. Chem Biol Drug Des;73:209–215.
21. Alves I.D., Goasdoué N., Correia I., Aubry S., Galanth C., Sagan S., Lavielle S., Chassaing G. (2008) Membrane interaction and perturbation mechanisms induced by two cationic cell penetrating peptides with distinct charge distribution. Biochim Biophys Acta;1780:948–959.
22. Bahnsen J.S., Franzyk H., Sandberg-Schaal A., Nielsen H.M. (2013) Antimicrobial and cell-penetrating properties of penetratin analogs: effect of sequence and secondary structure. Biochim Biophys Acta;1828:223–232.
23. Olivella M.S., Rodríguez A.M., Zacchino S.A., Somlai C., Penke B., Farkas V., Perczel A., Enriz R.D. (2010) New antifungal peptides. Synthesis, bioassays and initial structure prediction by CD spectroscopy. Bioorg Med Chem Lett;20:4808–4811.
24. Garibotto F.M., Garro A.D., Rodríguez A.M., Raimondi M., Zacchino S.A., Perczel A., Somlai C., Penke B., Enriz R.D. (2011) Penetratin analogues acting as antifungal agents. Eur J Med Chem;46:370–377.
25. Garibotto F.M., Garro A.D., Masman M.F., Rodríguez A.M., Luiten P.G.M., Raimondi M., Zacchino S.A., Somlai C., Penke B., Enriz R.D. (2010) New small-size peptides possessing antifungal activity. Bioorg Med Chem;18:158–167.
26. Garro A.D., Garibotto F.M., Rodriguez A.M., Raimondi M., Zacchino S.A., Perczel A., Somlai C., Penke B., Enriz R.D. (2011) New small-size antifungal peptides: design, synthesis and antifungal activity. Lett Drug Des Discovery;8:562–567.
27. Kaiser E., Colescott R.L., Bossinger C.D., Cook P.I. (1970) Color test for detection of free terminal amino groups in the solid-phase synthesis of peptides. Anal Biochem;34:595–598.
28. National Committee for Clinical and Laboratory Standards (NCCLS). (2008) Performance Standards for Antimicrobial Susceptibility Testing, 8th Informational Supplement, Document M100-S18. Wayne, PA: NCCLS.
29. Lima B., López S., Luna L., Agüero M.B., Aragón L., Tapia A., Zacchino S., López M.L., Zygadlo J., Feresin G.E. (2011) Essential oils of medicinal plants from the central andes of Argentina: chemical composition, and antifungal, antibacterial, and insect-repellent activities. Chem Biodivers;8:924–936.
30. Berendsen H.J.C., van der Spoel D., van Drunen R. (1995) GROMACS: a message-passing parallel molecular dynamics implementation. Comput Phys Commun;91:43–56.
31. Jorgensen W.L., Chandrasekhar J., Madura J.D., Impey R.W., Klein M.L. (1983) Comparison of simple potential functions for simulating liquid water. J Chem Phys;79:926–935.
32. Van Buuren A.R., Berendsen H.J.C. (1993) Molecular dynamics simulation of the stability of a 22-residue-helix in water and 30% trifluoroethanol. Biopolymers;33:1159–1166.
33. Berendsen H.J.C., Postma J.P.M., van Gunsteren W.F., Hermans J. (1981) Interaction models for water in relation to protein hydration. In: Pullman B., editor. Intermolecular Forces. Dordrecht, Holland: Reidel; p. 331–342.
34. Darden T., York D., Pedersen L. (1993) Particle mesh Ewald: an N·log(N) method for Ewald sums in large systems. J Chem Phys;98:10089–10092.
35. Zimmerman K. (1991) ORAL: all purpose molecular mechanics simulator and energy minimizer. J Comput Chem;12:310–319.

36. Berendsen H.J.C., Postma J.P.M., Van Gunsteren W.F., Dinola A., Haak J.R. (1984) Molecular dynamics with coupling to an external bath. J Chem Phys;81:3684–3690.
37. Miyamoto S., Kollman P.A. (1992) Settle: an analytical version of the SHAKE and RATTLE algorithm for rigid water models. J Comput Chem;13:952–962.
38. Hess B., Bekker H., Berendsen H.J.C., Fraaije J.G.E.M. (1997) LINCS: a Linear Constraint Solver for molecular simulations. J Comput Chem;18:1463–1472.
39. Politzer P., Truhlar D.G. (1981) Chemical Applications of Atomic and Molecular Electrostatic Potentials. New York: Plenum Press.
40. Náray-Szabó G., Ferenczy G.G. (1995) Molecular electrostatics. Chem Rev;95:829–847.
41. Chorev M., Goodman M. (1993) A dozen years of retro-inverso peptidomimetics. Acc Chem Res;26:266–273.
42. Jameson B.A., McDonnell J.M., Marini J.C., Korngold R. (1994) A rationally designed CD4 analogue inhibits experimental allergic encephalomyelitis. Nature;368:744–746.
43. Salamon Z., Lindblom G., Tollin G. (2003) Plasmon-waveguide resonance and impedance spectroscopy studies of the interaction between penetratin and supported lipid bilayer membranes. Biophys J;84:1796–1807.
44. Yesylevskyy S., Marrink S.J., Mark A.E. (2009) Alternative mechanisms for the interaction of the cell-penetrating peptides penetratin and the TAT peptide with lipid bilayers. Biophys J;97:40–49.
45. Bellet-Amalric E., Blaudez D., Desbat B., Graner F., Gauthier F., Renault A. (2000) Interaction of the third helix of Antennapedia homeodomain and a phospholipid monolayer, studied by ellipsometry and PM-IRRAS at the air-water interface. Biochim Biophys Acta;1467:131–143.
46. Letoha T., Gaá S., Somlai C., Czajlik A., Perczel A., Penke B. (2003) Membrane translocation of penetratin and its derivatives in different cell lines. J Mol Recognit;16:272–279.
47. Czajlik A., Meskó E., Penke B., Perczel A. (2002) Investigation of penetratin peptides. Part 1. The environment dependent conformational properties of penetratin and two of its derivatives. J Pept Sci;8:151–171.
48. Fischer P.M., Zhelev N.Z., Wang S., Melville J.E., Fahraeus R., Lane D.P. (2000) Structure-activity relationship of truncated and substituted analogues of the intracellular delivery vector Penetratin. J Pept Res;55:163–172.
49. Strøm M.B., Haug B.E., Skar M.L., Stensen W., Stiberg T., Svendsen J.S. (2003) The pharmacophore of short cationic antibacterial peptides. J Med Chem;46:1567–1570.
50. Findlay B., Zhanel G.G., Schweizer F. (2010) Cationic amphiphiles, a new generation of antimicrobials inspired by the natural antimicrobial peptide scaffold. Antimicrob Agents Chemother;54:4049–4058.

Notes

[a]Frisch M.J. *et al.* GAUSSIAN 03, Revision B.01, Gaussian, Inc.: Wallingford, CT, 2004.
[b]Flükiger P., Lüthi H.P., Portmann S., Weber, J. MOLEKEL 4.0. Swiss Center for Scientific Computing, Manno, Switzerland, 2000.

Supporting Information

Additional Supporting Information may be found in the online version of this article:

Figure S1. Change in the secondary structure during molecular dynamics simulations (100 ns) in water for (a) peptide **2**, (b) peptide **8**.

Figure S2. Change in the secondary structure during molecular dynamics simulations (100 ns) in TFE/water system for (a) peptide **1**, (b) peptide **2**, (c) peptide **8**.

Figure S3. Edmundson wheel representations of peptides **5** and **8**.